Chapter 1. Global agroclimatic patterns

Chapter 1 describes the CropWatch agroclimatic indicators for rainfall (RAIN), temperature (TEMP), and radiation (RADPAR), along with the agronomic indicator for potential biomass (BIOMSS) for sixty-five global Monitoring and Reporting Units (MRU). Rainfall, temperature, and radiation indicators are compared to their average value for the same period over the last fourteen years (called the "average"), while BIOMSS is compared to the indicator's average of the recent five years. Indicator values for all MRUs are included in Annex A, table A.1. For more information about the MRUs and indicators, please see Annex C and online CropWatch resources at www.cropwatch.com.cn.

As mentioned already in the November 2015 CropWatch Bulletin, the global patterns of rainfall anomalies that have been affecting the globe over the recent six months are largely conditioned by the on-going El Niño.

Large and consistent areas of anomalies are particularly clear throughout Eurasia and Africa (Figure 1.1 through 1.3). The MRU with the largest departure from average is the Western Cape in South Africa (MRU-10) where the recorded rainfall of 36 mm over the period is 68% below average, indicating a dry termination of the winter crop season in the part of South Africa that has a Mediterranean climate.

MRU-10 is part of a region that also includes MRU-09 (southern Africa), where the rainfall deficit was 23%, as well as the two Malagasy MRUs MRU-05, 'main', and MRU-06, semi-arid south-western Madagascar, where the deficit reached 10% and 29%, respectively. The area experienced slightly below average temperature (-0.1°C) but above average sunshine (+3.5%) and the deficit of biomass accumulation potential (-24%) indicates poor prospects for the on-going summer crops, especially maize, in this region (Figure 1.4 and sections 5.1 and 5.2).

North Africa-Mediterranean (MRU-07) and Mediterranean Europe and Turkey (MRU-59) are among the next most serious rainfall deficit areas with -53% and -31% departures from average, respectively. During the reporting period, both MRUs have been planting winter crops under relative water stress conditions.

Next come three areas with large rain deficits that can be described as "Punjab to Gujarat", "Southern Chinese Islands to New Zealand" and "Amazon-Patagonia". Punjab to Gujarat (MRU-48, rainfall deficit of -37%) is an isolated dry area in southern Asia, while the second spans the large area from MRU-42 (Taiwan, rainfall deficit of -34%) and MRU-33 (Hainan, rainfall deficit of -27%) via MRU-49 (maritime Southeast Asia, -24%) to MRU-53 (Northern Australia, rainfall deficit of -43%) and New Zealand (MRU-56,rainfall deficit of-65%). The area also includes East Asia (MRU-43, rainfall deficit of-29%) as well as Southern Japan and Korea (MRU-46, rainfall deficit of-13%).

The Amazon-Patagonia area is not continuous but encompasses large stretches of the Northern-central Andes (MRU-21, rainfall deficit of-21%), much of the Amazon basin (MRU-24, rainfall deficit of-32%) as well as Western Patagonia (MRU-27, rainfall deficit of-56%). This area is bordering the Pampas (rainfall surplus of +62%) and other agriculturally less important areas that, nevertheless, underwent unusually favourable conditions, such as central-North Argentina (MRU-25, rainfall surplus of +38%) and the Semi-arid Southern Cone (MRU-28, rainfall surplus of +50%).

North America was generally wet as a result of higher rainfall rates(MRU-12, Northern Great Plains, 56%; MRU-14, Cotton Belt to Mexican Nordeste, +61% and MRU-18, southwest USA and north Mexican highlands, +71%) with the exception of the west coast (MRU-16, -25%).

Conditions were close to average in Western Europe as well as northern Eurasia.

The wettest areas were part of a large portion of land that was already identified in the November 2015 CropWatch Bulletin, which encompasses many arid and semi-arid areas between West Africa and East Asia across most of Central Asia ("West Africa to East Asia wet area", WAEAWA). The largest positive rainfall departures occurred in Southern Mongolia (MRU-47, +272%) and in China (MRU-32, Gansu-Xinjiang, +139%; MRU-35, Inner Mongolia, +122% and MRU37, Lower Yangtze, +110%). They continue across Huanghuaihai (China, MRU-34), Northeast China (MRU-38), the Loess region (MRU-36), Southwest China (MRU-41), Southern China (MRU-40), the Pamir area (MRU-30, +102%), Western Asia (MRU-31, +42%), the Ural to Altai mountains (MRU-62, +41%), and eventually the Sahara to Afghan deserts (MRU-64, +50%) and the west African Sahel (MRU-08, 55%).

Figure 1.1. Global map of October 2015-January 2016 rainfall anomaly (as indicated by the RAIN indicator) by MRU, departure from 14YA (percentage)

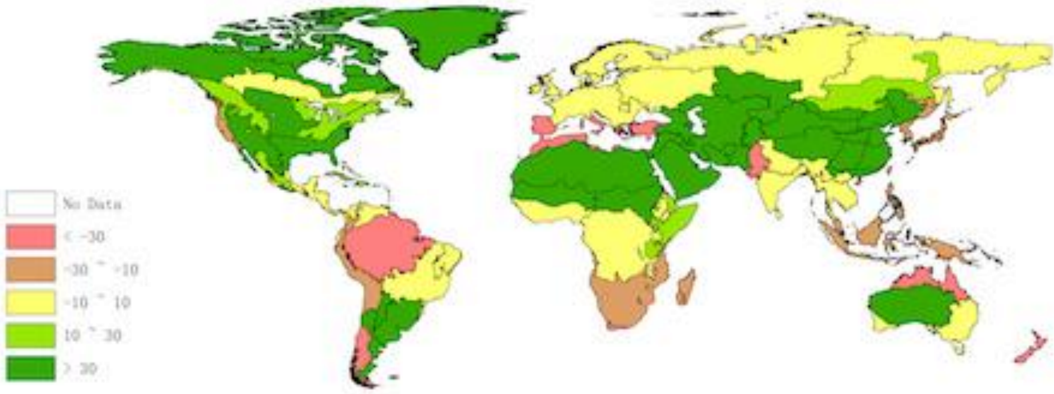

There is some consistency between the global patterns of rainfall and those of the other agroclimatic indicators, especially with regards to BIOMSS (Figure 1.4) and in particular with regard to the above-mentioned WAEAWA (Figure 1.2). The area also experienced generally low sunshine (less than 3% below average) and close to average positive temperature departures (close to +0.5°C).

Figure 1.2. Global map of October 2015-January 2016 air temperature anomaly (as indicated by the TEMP indicator) by MRU, departure from 14YA (degrees Celsius)

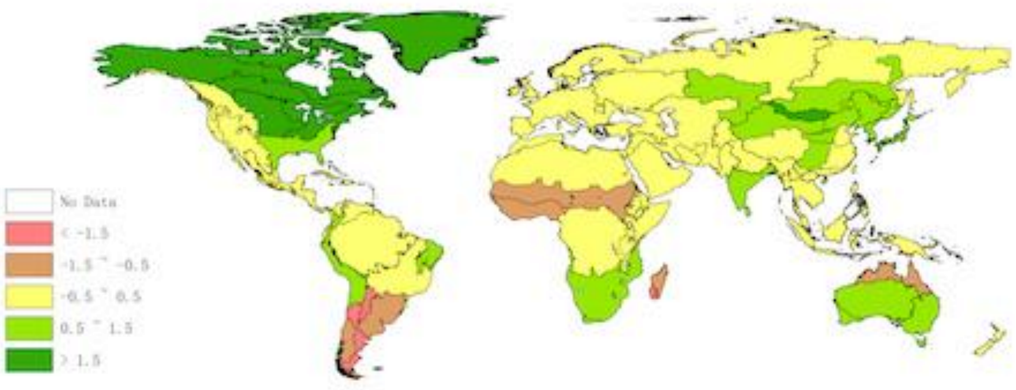

Particularly in the east, however, some areas had unusually low sunshine as shown by the RADPAR map (Figure 1.3): the Lower Yangtze (MRU-37, -22%), Southern China (MRU-40, -14%), Southwest China (MRU-41, -10%) and Huanghuaihai (MRU-34, -9%). Parallel departure patterns are recognizable in North America (Boreal America, MRU-61, -13%; Cotton Belt to Mexican Nordeste, MRU-14, -9%) and in the south of the continent (Pampas, MRU-26, -14% and Central-north Argentina, MRU-25, -11%).

Figure 1.3. Global map of October 2015-January 2016 PAR anomaly (as indicated by the RADPAR indicator) by MRU, departure from 14YA (percentage)

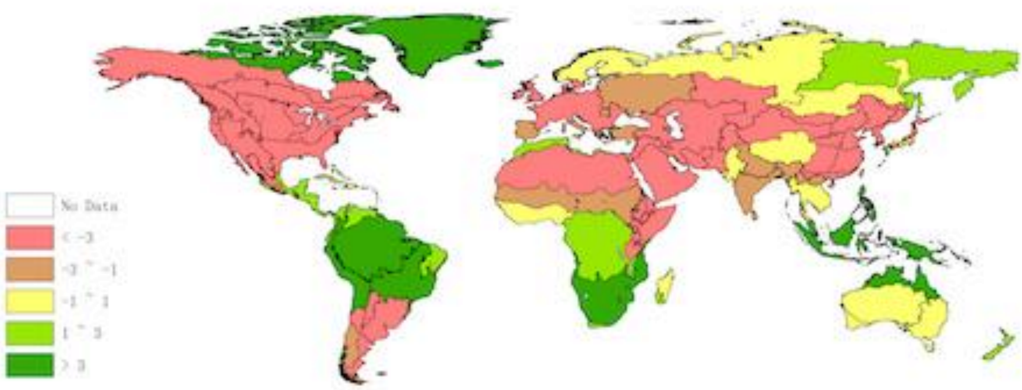

The most significant negative temperature departures occurred in precisely the same areas in South America (central-North Argentina, MRU-25, -2.0°C; Pampas, MRU-26, -1.3°C as well as the neighbouring semi-arid Southern Cone, MRU-28, -2.2°C), in Southwest Madagascar (MRU-06, -1.5°C) and in the Sahel (MRU-08, -1.0°C). Positive temperature departures were notable in areas that grow at least some winter crops (Cotton Belt to Mexican Nordeste, MRU-14, +1.5°C; Northern Great Plains, MRU-12, +2.0°C; Corn Belt, MRU-13, +2.3°C) but mostly at high latitudes with negative average temperature such as Boreal America (MRU-61, +2.9°C), Sub-boreal America (MRU-15, +2.9°C) and Sub-arctic America (MRU-65, +4.6°C). In Asia, the largest positive departure occurred in the Southern Mongolian MRU (MRU-47, +1.8°C).

Figure 1.4. Global map of October 2015-January 2016 biomass accumulation (BIOMSS) by MRU, departure from 5YA, (percentage)